Ranges of Cervical Intervertebral Disc Deformation During an In Vivo Dynamic Flexion–Extension of the Neck

Yan Yu

Department of Spine Surgery,
Tongji Hospital,
Tongji University School of Medicine,
Shanghai 2000065, China;
Department of Orthopedic Surgery,
Massachusetts General Hospital,
Harvard Medical School,
Boston, MA 02114

Haiqing Mao

Department of Orthopedic Surgery,
The First Affiliated Hospital of Soochow University,
Suzhou 215006, Jiangsu, China

Jing-Sheng Li

College of Health and Rehabilitation Sciences,
Sargent College,
Boston University,
Boston, MA 02215

Tsung-Yuan Tsai

School of Biomedical Engineering,
Shanghai Jiao Tong University,
Shanghai 200030, China

Liming Cheng

Department of Spine Surgery,
Tongji Hospital,
Tongji University School of Medicine,
Shanghai 200065, China

Kirkham B. Wood

Department of Orthopaedic Surgery,
Stanford University Medical Center,
Redwood City, CA 94063

Guoan Li[1]

Department of Orthopedic Surgery,
Massachusetts General Hospital,
Harvard Medical School,
55 Fruit Street, GRJ 1215,
Boston, MA 02114
e-mail: guoanli12@gmail.com

Thomas D. Cha

Department of Orthopedic Surgery,
Massachusetts General Hospital,
Harvard Medical School,
Boston, MA 02114

While abnormal loading is widely believed to cause cervical spine disc diseases, in vivo cervical disc deformation during dynamic neck motion has not been well delineated. This study investigated the range of cervical disc deformation during an in vivo functional flexion–extension of the neck. Ten asymptomatic human subjects were tested using a combined dual fluoroscopic imaging system (DFIS) and magnetic resonance imaging (MRI)-based three-dimensional (3D) modeling technique. Overall disc deformation was determined using the changes of the space geometry between upper and lower endplates of each intervertebral segment (C3/4, C4/5, C5/6, and C6/7). Five points (anterior, center, posterior, left, and right) of each disc were analyzed to examine the disc deformation distributions. The data indicated that between the functional maximum flexion and extension of the neck, the anterior points of the discs experienced large changes of distraction/compression deformation and shear deformation. The higher level discs experienced higher ranges of disc deformation. No significant difference was found in deformation ranges at posterior points of all the discs. The data indicated that the range of disc deformation is disc level dependent and the anterior region experienced larger changes of deformation than the center and posterior regions, except for the C6/7 disc. The data obtained from this study could serve as baseline knowledge for the understanding of the cervical spine disc biomechanics and for investigation of the biomechanical etiology of disc diseases. These data could also provide insights for development of motion preservation surgeries for cervical spine.
[DOI: 10.1115/1.4036311]

Keywords: cervical spine, spine disc, disc deformation, in vivo spine kinematics, disc degeneration

Introduction

Cervical spine disc diseases are common among adults and reach a prevalence of nearly 95% by the age of 65 yr [1]. Neck pain is the most frequently seen symptom in clinic [2,3] and is commonly attributed to cervical disc diseases [4]. In severe conditions, disc diseases can result in instability, neurologic deficit, spinal stenosis, facet dysfunction, and less cervical lordosis [5–9]. These clinical symptoms can lead to loss of the neck motion and cause disability to patients [7–9]. Despite various biological factors that have been related to disc diseases [10–13], abnormal spinal motion and the consequent abnormal loading have been widely assumed to be the etiology of spinal pathology [14,15]. Therefore, understanding of the spinal biomechanics is critically important for investigation of the mechanisms of cervical spine disc diseases and for development of treatment modalities to restore neck function. However, a literature review indicated that few studies have been reported on the biomechanics of the cervical spine discs [16]. For example, sagittal plane magnetic resonance (MR) or plane X-ray images have been used to investigate disc space heights at nonweightbearing supine or weightbearing standing positions [17–20]. Three-dimensional (3D) finite element modeling methods have been used to study cervical disc deformation under various simulated loading conditions [21–26]. Cervical interverterbral kinemeatics has also been investigated by using in vitro human cadaveric models [27–30] and in vivo human subjects [15,31–35].

While these studies have greatly improved our knowledge on cervical spine biomechanics, few data have been reported on the in vivo cervical disc deformation under physiological, dynamic loading conditions [36,37]. Since the cervical spine experiences the largest range of motion along the spine column, it is critically important to understand the biomechanical roles of the discs during the neck motion for investigation of clinically relevant issues of the cervical spine. For instance, the mechanisms of commonly observed higher rate of C5/6 degeneration than C6/7 in clinic are not well investigated; the mechanisms of postoperative adjacent segment degeneration following intervertebral fusion are still debated.
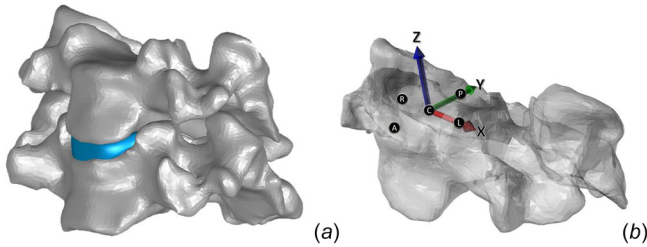
(a)   (b)

Fig. 1 The disc coordinate system and the locations on the disc surface: A—anterior, C—center, P—posterior, L—left, and R—right points

Therefore, the objective of this study was to investigate the physiological geometric deformation of human cervical spine discs during functional neck motions. We have previously utilized a combined dual fluoroscopic imaging system (DFIS) and MRI-based 3D modeling technique to investigate human lumbar disc deformation [38,39]. In this study, we investigated the range of cervical spine disc deformation of asymptomatic human subjects during dynamic, full range flexion–extension motion of the neck. We hypothesized that the physiological cervical disc deformation is segmental level dependent and the C5/6 disc experiences higher deformation than the C6/7 disc.

Materials and Methods

Subject Recruitment. This study was approved by our Institutional Review Board (IRB) and each patient signed an informed consent prior to participation. Ten asymptomatic subjects with an average of 40.3 ± 10.9 yr old (six males and four females, average body mass index 24.6 ± 3.2 kg/m^2) were recruited from one academic center. Each subject was first evaluated for the absence of neck pain and other spinal disorders by an experienced spine surgeon. Using MR images of the subject, the presence of any anatomic abnormalities, early disc degeneration was used as an exclusion factor from further investigation. Cervical disc deformations at the C3/4, C4/5, C5/6, and C6/7 segments of each subject were investigated (40 discs were studied totally).

MR-Based Three-Dimensional Model. The subject was scanned in a supine, relaxed position using a 3 T MR scanner (MAGNETOM Trio, Siemens, Erlangen, Germany) with a spine coil and a proton density weighted sequence. The MR images were used to construct 3D models of the vertebrae from C3 to C7 [40]. C1 and C2 were not modeled in this study because they might be obscured by the skull and mandible in the experimental setup. The contours of the vertebrae were digitized using the 3D slicer modeling software (3D SLICER; MIT Artificial Intelligence Lab and Brigham and Women's Hospital, Boston, MA) [41]. The disc was represented by the interspace between the adjacent cervical endplates (Fig. 1(a)).

Dual Fluoroscopic Imaging Procedure. The cervical spine of the subject was imaged dynamically from a maximum flexion to maximum extension of the neck using the DFIS. The DFIS consists of two fluoroscopes (BV Pulsera®, Phillips, Bothell, WA) that were positioned with image intensifiers perpendicular to each other. The two fluoroscopes captured cervical images simultaneously from two orthogonal directions while the subject sat on a chair to keep the trunk stable and moved the neck within the field of view of the two fluoroscopes. The subject was imaged as the neck extended from a full flexion to full extension position and flexed back to the original position. The positions of the C3–C7 segments were captured along the motion path by the fluoroscopes at 30 frames per second. Each subject was exposed to a radiation dosage of ~ 0.08 mSv.

Reproduction of In Vivo Cervical Kinematics. The pair of fluoroscopic images captured during dynamic neck motion was imported into the software (Rhinoceros®, Robert McNeel & Associates, Seattle, WA) and placed in calibrated virtual orthogonal planes to construct a virtual dual fluoroscopic system. The 3D MR-based models of the cervical vertebrae were introduced into this virtual system and were independently translated and rotated in six degrees-of-freedom (6DOF) until their contours matched those captured on the two fluoroscopic images to reproduce the in vivo vertebral positions (Fig. 2). The in vivo positions of the cervical vertebrae at the maximum flexion and extension positions were reproduced for investigation of the range of motion of each intervertebral level and the range of disc deformation during the maximum flexion–extension of the neck. A validation of this technique in determination of intervertebral kinematics has been performed by comparing our model matching data with those obtained using roentgen stereophotogrammetric analysis (RSA) technique (see the Appendix). The mean accuracy in vertebral translation measured using the root-mean-square error (RMSE)
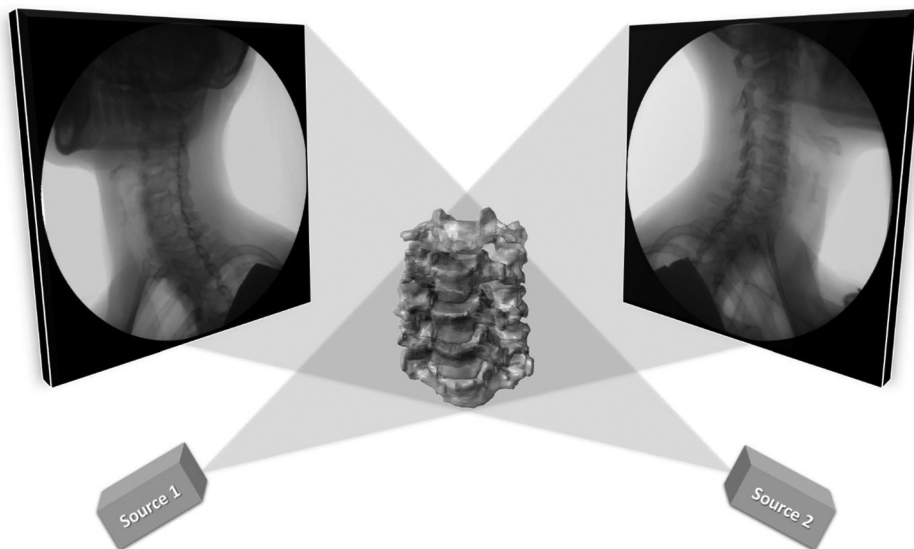

Fig. 2 The virtual DIFS for reproduction of the in vivo cervical vertebrae positions

was 0.54 mm in the superoinferior and anteroposterior directions of the intervertebral disc (see Table 3 in the Appendix).

Disc Deformation Calculation. The geometry of the intervertebral disc during the functional activity was calculated using the relative positions of the upper and lower endplates of each intervertebral segment (C3/4, C4/5, C5/6, and C6/7). Overall disc deformation was determined using the changes of the intervertebral segment space geometry where the cervical spine position obtained during MRI scanning was used as a nonweightbearing reference for the calculation of disc deformation [38].

To examine the inhomogeneous deformation and simplify the analysis, the continuum of disc regions illustrated in Fig. 3 was broken down into five specific mesh vertices on the disc surface: anterior, central, posterior, left, and right points of the disc (Fig. 1(b)). Local disc height was defined using the MRI neck position at each vertices of the superior endplate and was calculated using the iterative closest point method [38]. Disc height vector was defined as the vector between the superior and inferior endplates. The change of the disc height during neck motion was calculated as the vectorial difference between the disc height vectors at a dynamic disc position and at the MRI scanning position in the

disc coordinate system (Fig. 1(b)). The overall deformation of the disc was calculated by normalizing the change of dynamic disc height using the disc height measured at the MRI scanning position for each local area [38]. The overall distraction/compression deformation at each point was defined as the component of change of disc height vector perpendicular to the distal endplate (z-axis); the shear deformation was defined as the component of change of disc height vector parallel to the plane of the distal endplate (x–y plane). In this study, the changes of disc deformation between the maximum extension and flexion positions were defined as the differences between the overall deformations of the discs at the two neck positions. Both the ranges of disc deformation between flexion to extension and extension to flexion were calculated and averaged to represent the ranges of disc deformation between the maximum flexion and extension positions of the discs.

Data Analysis. The disc height and range of motion among different levels were analyzed using an analysis of variance (ANOVA) method. The changes of the magnitudes of distraction/compression and shear deformations between the maximum extension and flexion positions were analyzed. A repeated-measure ANOVA was used to compare the disc deformations at the four intervertebral levels and five locations inside the discs (20 times in total). A post hoc Newman–Keuls test was performed when significant difference was detected. The level of significance was set at 0.05 for all the tests.

Results

Disc Height and Range of Motion. The height of the cervical discs at MRI scan position changed from 3.5 to 4.9 mm and varied with levels and locations (Table 1). The anterior height decreased from C6/7 to C3/4, whereas the opposite situation was observed at the posterior points. No significant difference, however, was detected among the different intervertebral discs ($P > 0.05$). The C3/4 height increased progressively from anterior to posterior (3.8–4.6 mm), but the C6/7 showed an opposite trend (4.9–3.8 mm). The disc height at the center point is lower than at the anterior and posterior points at C4/5 and C5/6. In general, no statistically significant difference was found among the measures at these discrete locations. During the maximum flexion–extension, C3/4, C4/5, and C5/6 had similar ranges of motion with averages between 14 and 17 deg. The C6/7 had a range of motion of 9.4 ± 4.2 deg that was significantly lower than the higher level segments ($P < 0.05$).

Changes of Disc Deformation Between the Maximum Extension and Flexion Positions. Calculated overall disc deformations of C3/4 of a typical subject are shown in Fig. 3. At maximum flexion, the anterior portion of the disc experienced compression (blue) and the posterior part experienced tensile deformation (red). The condition was reversed at the maximum extension position of the neck. The shear deformation changed directions with the neck positions. Since similar data were observed among the center, left, and right points, only center point data were presented together with the anterior and posterior points.

Between the full flexion and extension of the neck, the anterior points of C3/4, C4/5, and C5/6 experienced similar changes of distraction/compression deformation ($70.3 \pm 34.1\%$, $61.9 \pm 28.8\%$, and $75.9 \pm 32.2\%$, respectively, $P > 0.05$) (Table 2). The C6/7 experienced a range of distraction deformation of $39.1 \pm 37.4\%$ that is significantly lower than those of the higher level discs ($P < 0.05$). At the center points of all the discs, the distraction/compression deformation changes between the flexion and extension neck positions were similar ($P > 0.05$). Similarly, the ranges of distraction/compression deformation of the posterior points of all the discs were not significantly different ($P > 0.05$).

In general, the change of deformation at the center point of each disc is significantly lower than those at the anterior points ($P < 0.05$) except for C6/7 and posterior points ($P < 0.05$) except
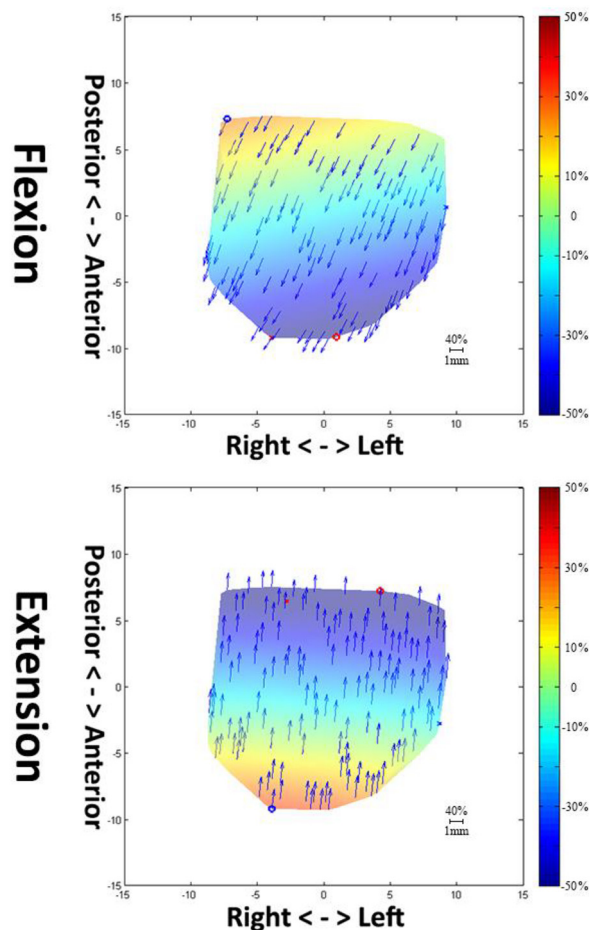

Fig. 3 Distraction/compression (color) and shear (arrows) deformation are normalized to disc height (expressed by percentage of the disc height) of the C3/4 disc in a typical subject at the maximum flexion and extension neck positions. In the color code, 50% indicates a distraction that is 50% of the disc height and −50% indicates a compression that is 50% of the disc height. The arrows indicate the shear deformation direction and their magnitudes are represented by the arrow length. Scale bar (=1 mm) represents a shear deformation of 40% of the disc height. (Color figure can be viewed online)

Table 1 Local heights (mm) at discrete locations of the discs measured at the supine MRI scanning position of the subjects and range of motion of each vertebral level (deg) during full range of dynamic flexion–extension of the neck

| Disc level | Disc height | | | | | Range of motion during flexion–extension |
	Anterior	Center	Posterior	Left	Right	
C3/4	3.8 ± 1.0	4.1 ± 0.8	4.6 ± 1.0	4.1 ± 1.4	4.2 ± 0.8	14.6 ± 5.4
C4/5	4.1 ± 0.9	3.7 ± 0.9	4.6 ± 1.1	3.5 ± 0.8	4.0 ± 1.2	16.8 ± 5.3
C5/6	4.3 ± 0.9	4.1 ± 0.6	4.2 ± 0.7	4.0 ± 0.9	3.6 ± 0.9	15.2 ± 6.1
C6/7	4.9 ± 1.3	4.6 ± 0.9	3.8 ± 0.9	3.6 ± 0.9	3.9 ± 0.7	9.4 ± 4.2[a]

[a]Indicates significant difference between C6/7 and above segments.

Table 2 The changes (%) of the disc deformation between the maximum flexion and extension positions of the neck

| | Tensile deformation | | | Shear deformation | | |
	Anterior[a,b,c]	Center	Posterior	Anterior[a,b,c]	Center[a,b,d,e]	Posterior
C3/4[f,g,h]	70.3 ± 34.1	13.2 ± 12.6	37.5 ± 20.4	68.3 ± 34.1	57.8 ± 13.4	45.9 ± 16.8
C4/5[f,g]	61.9 ± 28.8	17.2 ± 14.4	50.9 ± 35.2	78.5 ± 41.3	76.7 ± 28.8	60.5 ± 31.5
C5/6[f,h]	75.9 ± 32.2	25.4 ± 23.1	40.4 ± 22.2	48.3 ± 20.9	46.0 ± 16.5	42.9 ± 17.9
C6/7	39.1 ± 37.4	21.5 ± 19.8	34.4 ± 25.5	33.1 ± 18.2	30.9 ± 14.7	34.6 ± 14.5

Note: Significant differences between different intervertebral levels when $P < 0.05$: [e]for C3/4 versus C4/5, [b]for C3/4 versus C6/7, [d]for C4/5 versus C5/6, [a]for C4/5 versus C6/7, and [c]for C5/6 versus C6/7. Significant differences between different locations (anterior, center, and posterior points) of the disc when $P < 0.05$: [f]for anterior versus center, [g]for center versus posterior, and [h]for anterior versus posterior. No significant difference was detected in shear deformation.

for C5/6 and C6/7. No statistically significant difference was observed at different points of the C6/7.

Between maximum flexion and extension of the neck, the anterior points of C3/4, C4/5, and C5/6 experienced similar changes of shear deformation (68.3 ± 34.1%, 78.5 ± 41.3%, and 48.3 ± 20.9%, respectively, $P > 0.05$) (Table 2), which are significantly higher than that of C6/7 (33.1 ± 18.2%, $P < 0.05$). The change of shear deformation at the center point of C4/5 (76.7 ± 28.8%) was significantly higher than those of C3/4, C5/6, and C6/7 (57.8 ± 13.4%, 46.0 ± 16.5%, and 30.9 ± 14.7%, respectively) ($P < 0.05$), and the change of C3/4 was found to be higher than that of C6/7 ($P < 0.05$). At the posterior points, no significant difference in changes of shear deformation was observed among the discs. No significant difference in the changes of shear deformation was observed between the different locations of each disc.

Discussion

This study investigated the ranges of in vivo cervical spine disc deformation of asymptotic subjects between functional maximum flexion and extension positions of the neck using a combined DFIS and 3D MRI-based modeling technique. The data showed that the cervical spine experienced large range of distraction/compression and shear deformations between the two neck positions. The disc deformation varied with intervertebral levels in both distraction/compression and shear deformations, especially at the anterior points. The distraction/compression deformation also varied from anterior to posterior points inside the same disc, but less with the intravertebral locations for shear deformation.

Several studies have reported on the cervical spine disc heights using sagittal plane MRI or X-ray images [17–19]. These studies indicated that on average, the disc height varies between 3.2 and 5.2 mm. These data, in general, were consistent with our measures. Our data indicated that while there are variations in disc heights within the disc and among different disc levels, the cervical spine discs are around 4.2 mm in heights when the neck is at a nonweightbearing supine position.

Various in vitro and in vivo studies [31–35,42–44] have investigated the cervical spine kinematics under various external loading conditions, but few data have been reported on the physiological cervical disc deformation during dynamic neck motion. Most of the studies on disc biomechanics used finite element modeling

methods and few reported the data of disc deformation [21,45]. For example, del Palomar et al. simulated the cervical spine biomechanics from C2 to C7 under a static compressive load of 50 N and reported a maximum shear deformation of 30% [21]. Goel and Clausen determined the distraction strain of the anterior longitudinal ligament (ALL) that is located close to the anterior margin of disc and reported a 10.1% peak strain when the cervical spine was under a 73.6 N compression accompanied with a 1.8 N·m extension torque [45]. Anderst et al. studied the in vivo cervical disc deformation during dynamic neck motion using a combined computed tomography-biplane X-ray system and reported a peak deformation of 47.8 ± 4.4% at the posterior-lateral region, followed by a 24.6 ± 2.7% at anterior region and a 6.9 ± 0.9% at central nucleus among all the disc levels [36]. Our data indicated that on average, some locations inside the discs, especially at the anterior region, could experience changes of distraction/compression and shear disc deformation over 70%. The differences between our data and those in vitro data reported in literature could be due to the differences between the in vivo physiological cervical loading conditions and the loading conditions simulated in in vitro experimental or numerical studies [21,23,24,27]. Anderst et al. used a standing neutral, weightbearing position as the reference to calculate disc deformation while we used the nonweightbearing, supine position as the reference. Therefore, it is difficult to directly compare the data of different studies.

The data of this paper indicated that the cervical spine disc experiences large deformation during physiological activities and different discs responded to neck motion differently. While the C3/4, C4/5, and C5/6 discs experienced a change of disc deformation above 60% at the anterior points between the full flexion and extension positions of the neck, the anterior point of C6/7 experienced a much lower change of disc deformation compared to the above segments with almost similar disc deformation changes at the posterior and anterior points. Therefore, any simulation of disc function of the cervical spine, either at organic or at cellular level, may need to consider the large range of physiological deformation experienced by the discs. Simulation of disc deformation in 10–30% strain level using numerical techniques [21,45] corresponds to a small range of neck motion that could underestimate the in vivo disc function and provide insufficient data to the development of clinical diagnosis and therapy as well as the development of internal transplantations.

These observations could also have other interesting clinical relevance. In literature, cervical disc diseases were mostly reported at C5/6, followed by at C6/7 and then C4/5 [46,47]. Our data revealed that there is a large difference between the C4/5, C5/6, and C6/7 in distraction/compression and shear disc deformation patterns. The distraction/compression deformations of the C4/5 and C5/6 are significantly higher at the anterior points than at the central, but for C6/7, no significant difference was observed within the disc. The ranges of disc deformations at the anterior points of C4/5 and C5/6 are almost twice of that of C6/7. Although the shear deformations of C4/5 and C5/6 at the anterior point were also significantly different from that of C6/7, the C4/5, on average, had shear deformation almost two times larger than both the C5/6 and C6/7. This dramatic transition in disc biomechanics among these discs might play a role in the clinically observed prevalence of disc diseases at these three segments. A future study is warranted to investigate the relationship between the biomechanical features of the discs and their pathogenesis development.

In treatment of severe cervical disc diseases, disc fusion is the most commonly used surgical procedures. However, postoperative adjacent segment degeneration has often been reported [48]. With disc deformation changes up to 70% at C5/6 and up to 40% at C6/7 during functional neck activities, fusion of either discs might alter the structural properties of the spine and cause changes in biomechanical environment at the adjacent levels. It is therefore important to quantitatively investigate the effect of fusion surgeries on the changes of biomechanics of adjacent segments and to examine if there is a relationship between the biomechanical changes of the cervical spine after surgical fusion and the adjacent segment degeneration.

Motion preservation disc replacement has been increasingly used in treatment of severe disc diseases [49,50]. However, this surgery does not significantly reduce the postoperative complication rates when compared to fusion surgeries [50]. Numerous studies have investigated the cervical spine kinematics after disc replacement surgeries [27,51–53]. Using cadaveric studies with a biomechanical hybrid testing protocol, Dmitriev et al. measured the adjacent level intradiscal pressure following a total replacement arthroplasty using a custom-designed spine simulator that allows pure, unconstrained multidirectional load application [27]. The adjacent disc pressure was shown to increase by 5% and 21% in the proximal and distal adjacent levels, respectively. Using a 3D finite element modeling technique, the adjacent disc motion showed similar kinematics to the normal cervical spine model [53]. Motion preservation devices could improve the segment motion at index level under simulated loading conditions, but they might not preserve the loading capacities or deformation characters of the adjacent discs. Recent perspective randomized control trails comparing arthroplasty and arthrodesis have presented safety as well as equal or better clinical outcomes [54]. Future investigation of cervical arthroplasty and arthrodesis may need to consider the level-dependent deformation characters of the cervical discs under physiological conditions.

There are several limitations to the current study. The analysis of the disc deformation was limited to the subaxial cervical spine. The C1/2 and C2/3 were not included due to the possible obstruction of their images by the mandibular and occipital bones in certain postures along the neck motion path. We found it is a challenge to determine a neck position as the true, unique reference to calculate disc deformation. The MR supine position of the neck was used as a reference position to calculate the disc height. This may not represent the true reference position. Therefore, we only investigated the changes of disc deformation between the full flexion and extension positions of the neck. The overall geometric deformation was calculated, and no deformation inside the disc was presented. Future study should focus on investigation of in vivo stress–strain distributions inside the discs using 3D finite element modeling of the discs, which uses the overall geometric deformation as boundary conditions. Finally, only ten asymptomatic subjects were investigated within the age distribution ranging from 30 to 59 yr old. In the future, more subjects with a wide range of age should be included to clarify the effects of age on cervical disc biomechanics.

Conclusion

The overall intervertebral disc deformation of the subaxial cervical spine was investigated during a maximum flexion–extension of the neck. The changes of the disc deformation between the maximum flexion and extension positions of the neck were segment level dependent and disc location dependent and could reach over 70% in cervical spine discs. These data could provide boundary conditions for other researchers who use finite element (FE) models to investigate in vivo disc stress–strain responses to functional activities. The overall disc deformation data could also be instrumental for those using ex vivo experiment to study cellular response of the disc tissue in response to physiological disc deformation. Further, this study could provide insights into improvement of fusion and disc replacement surgeries that are aimed to prevent adjacent segment degenerations after the surgery.

Acknowledgment

Appendix: Validation of the DFIS in Measurement of Cervical Spine Motion

Experimental Setup

A validation study was performed to evaluate the accuracy of the combined dual fluoroscopic imaging system (DFIS) and MRI modeling technique for measurement of dynamic intervertebral cervical spine motion.

One male fresh-frozen human cervical cadaveric specimen (age: 60 yr old; height: 182.9 cm; and weight: 46.7 kg) was dissected and implanted with four 2 mm metal beads in each vertebrae (Fig. 4). All the soft tissues surrounding the cadaver remained intact. In view of the DFIS, the cadaveric spine was manually moved throughout its range of motion during a series of dynamic activities, including flexion–extension, lateral side-bending, and twisting. The speed of the movements was
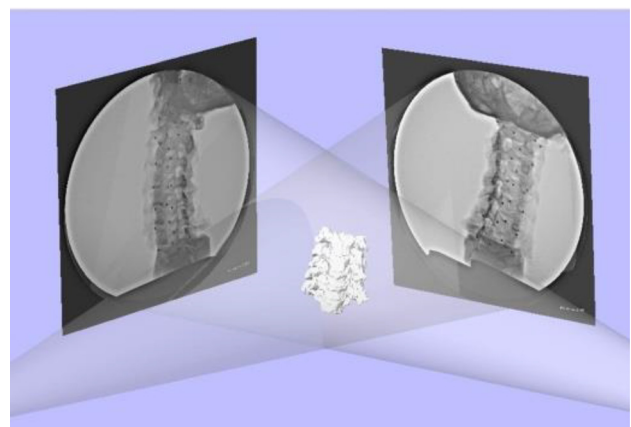

Fig. 4 Validation of the DFIS system in reproducing the in vivo vertebral positions. The RSA method using metal beads was used as the reference.

Table 3 RMSE in determining intervertebral kinematics at the C3/4, C4/5, C5/6, and C6/7 levels for each activity

Level	Activity	ML (mm)	AP (mm)	SI (mm)	FE (deg)	SB (deg)	Twist (deg)
C3/4	Flexion–extension	0.38	1.52	0.29	3.02	1.59	1.51
	Side bend	0.60	0.68	0.60	1.45	1.68	1.12
	Twist	0.66	0.61	0.42	1.88	0.71	1.33
C4/5	Flexion–extension	0.62	0.32	0.33	1.86	1.07	1.58
	Side bend	0.67	0.30	0.56	1.34	0.60	1.45
	Twist	0.47	0.21	0.20	0.48	0.98	1.73
C5/6	Flexion–extension	0.47	0.35	0.49	1.18	0.94	1.28
	Side bend	1.32	0.81	0.29	0.79	1.17	1.75
	Twist	0.64	0.43	0.59	1.09	0.95	0.88
C6/7	Flexion–extension	0.51	0.86	0.36	0.99	0.73	1.44
	Side bend	0.92	0.51	0.66	0.74	1.91	1.79
	Twist	0.78	0.70	0.73	0.64	1.20	2.10
Average		0.67	0.61	0.46	1.29	1.13	1.50

Note: ML, medial–lateral; AP, anterior–posterior; SI, superior–inferior; FE, flexion–extension; and SB = side bend.

performed under the beats of metronome, such that one full motion cycle took approximately 3 s. The fluoroscopes captured dynamic images of vertebrae at 30 frames per second with an 8 ms pulse-width.

Following fluoroscopy imaging, the cadaver model was MRI scanned for the construction of 3D vertebral models. The vertebrae models and fluoroscopy images were then used to recreate intervertebral kinematics in 6DOF at various points throughout the dynamic activities, as described in the "Materials and Methods" section. The results from the model-based combed MRI–DFIS technique were compared to those obtained using RSA, which is considered the gold standard in bone tracking. The accuracy of the DFIS technique was quantified in terms of root-mean-square error (RMSE).

Results

Table 3 displays the RMSE in determining intervertebral kinematics at the C3/4, C4/5, C5/6, and C6/7 levels for each activity. On average, the model matching technique was able to reproduce 6DOF dynamic intervertebral kinematics with an accuracy of 0.6 mm and 1.3 deg.

References

[1] Malcolm, G. P., 2002, "Surgical Disorders of the Cervical Spine: Presentation and Management of Common Disorders," J. Neurol. Neurosurg. Psychiatry, 73(Suppl. 1), pp. i34–i41.

[2] Baek, S. H., Oh, J. W., Shin, J. S., Lee, J., Lee, Y. J., Kim, M. R., Ahn, Y. J., Choi, A., Park, K. B., Shin, B. C., Lee, M. S., and Ha, I. H., 2015, "Long Term Follow-Up of Cervical Intervertebral Disc Herniation Inpatients Treated With Integrated Complementary and Alternative Medicine: A Prospective Case Series Observational Study," BMC Complementary Altern. Med., 16(1), p. 52.

[3] Bovim, G., Schrader, H., and Sand, T., 1994, "Neck Pain in the General Population," Spine, 19(12), p. 1307–1309.

[4] Avery, R. M., 2012, "Massage Therapy for Cervical Degenerative Disc Disease: Alleviating a Pain in the Neck?," Int. J. Ther. Massage Bodywork, 5(3), pp. 41–46.

[5] Yang, K. H., and King, A. I., 1984, "Mechanism of Facet Load Transmission as a Hypothesis for Low-Back Pain," Spine, 9(6), pp. 557–565.

[6] Gore, D. R., Sepic, S. B., and Gardner, G. M., 1986, "Roentgenographic Findings of the Cervical Spine in Asymptomatic People," Spine, 11(6), pp. 521–524.

[7] Suda, K., Abumi, K., Ito, M., Shono, Y., Kaneda, K., and Fujiya, M., 2003, "Local Kyphosis Reduces Surgical Outcomes of Expansive Open-Door Laminoplasty for Cervical Spondylotic Myelopathy," Spine, 28(12), pp. 1258–1262.

[8] Barsa, P., and Suchomel, P., 2007, "Factors Affecting Sagittal Malalignment Due to Cage Subsidence in Standalone Cage Assisted Anterior Cervical Fusion," Eur. Spine J., 16(9), pp. 1395–1400.

[9] Kawaguchi, Y., Kanamori, M., Ishihara, H., Ohmori, K., Nakamura, H., and Kimura, T., 2003, "Minimum 10-Year Followup After En Bloc Cervical Laminoplasty," Clin. Orthop. Relat. Res., 411, pp. 129–139.

[10] Roberts, S., Menage, J., and Urban, J. P., 1989, "Biochemical and Structural Properties of the Cartilage End-Plate and Its Relation to the Intervertebral Disc," Spine, 14(2), pp. 166–174.

[11] Bibby, S. R., Fairbank, J. C., Urban, M. R., and Urban, J. P., 2002, "Cell Viability in Scoliotic Discs in Relation to Disc Deformity and Nutrient Levels," Spine, 27(20), pp. 2220–2228; discussion 2227–2228.

[12] Chan, W. C., Sze, K. L., Samartzis, D., Leung, V. Y., and Chan, D., 2011, "Structure and Biology of the Intervertebral Disk in Health and Disease," Orthop. Clin. North Am., 42(4), pp. 447–464, vii.

[13] Wu, D. J., Chen, K., Wei, X. Z., Ni, H. J., Yu, S. Z., Zhu, X. D., and Li, M., 2014, "Analysis of Intervertebral Disc-Related Genes," Genet. Mol. Res., 13(1), pp. 2032–2038.

[14] Lin, R. M., Tsai, K. H., Chu, L. P., and Chang, P. Q., 2001, "Characteristics of Sagittal Vertebral Alignment in Flexion Determined by Dynamic Radiographs of the Cervical Spine," Spine, 26(3), pp. 256–261.

[15] Miyazaki, M., Hymanson, H. J., Morishita, Y., He, W., Zhang, H., Wu, G., Kong, M. H., Tsumura, H., and Wang, J. C., 2008, "Kinematic Analysis of the Relationship Between Sagittal Alignment and Disc Degeneration in the Cervical Spine," Spine, 33(23), pp. E870–E876.

[16] Anderst, W., 2016, "Narrative Review of the in vivo Mechanics of the Cervical Spine After Anterior Arthrodesis as Revealed by Dynamic Biplane Radiography," J. Orthop. Res., 34(1), pp. 22–30.

[17] Kolstad, F., Myhr, G., Kvistad, K. A., Nygaard, O. P., and Leivseth, G., 2005, "Degeneration and Height of Cervical Discs Classified From MRI Compared With Precise Height Measurements From Radiographs," Eur. J. Radiol., 55(3), pp. 415–420.

[18] Gilad, I., and Nissan, M., 1986, "A Study of Vertebra and Disc Geometric Relations of the Human Cervical and Lumbar Spine," Spine, 11(2), pp. 154–157.

[19] Kumaresan, S., Yoganandan, N., Pintar, F. A., Macias, M., and Cusick, J. F., 2000, "Morphology of Young and Old Cervical Spine Intervertebral Disc Tissues," Biomed. Sci. Instrum., 36, pp. 141–146.

[20] Frobin, W., Leivseth, G., Biggemann, M., and Brinckmann, P., 2002, "Vertebral Height, Disc Height, Posteroanterior Displacement and Dens-Atlas Gap in the Cervical Spine: Precision Measurement Protocol and Normal Data," Clin. Biomech., 17(6), pp. 423–431.

[21] del Palomar, A. P., Calvo, B., and Doblare, M., 2008, "An Accurate Finite Element Model of the Cervical Spine Under Quasi-Static Loading," J. Biomech., 41(3), pp. 523–531.

[22] Kallemeyn, N., Gandhi, A., Kode, S., Shivanna, K., Smucker, J., and Grosland, N., 2010, "Validation of a C2-C7 Cervical Spine Finite Element Model Using Specimen-Specific Flexibility Data," Med. Eng. Phys., 32(5), pp. 482–489.

[23] Womack, W., Leahy, P. D., Patel, V. V., and Puttlitz, C. M., 2011, "Finite Element Modeling of Kinematic and Load Transmission Alterations Due to Cervical Intervertebral Disc Replacement," Spine, 36(17), pp. E1126–E1133.

[24] Hussain, M., Natarajan, R. N., An, H. S., and Andersson, G. B., 2012, "Progressive Disc Degeneration at C5-C6 Segment Affects the Mechanics Between Disc Heights and Posterior Facets Above and Below the Degenerated Segment: A Flexion-Extension Investigation Using a Poroelastic C3-T1 Finite Element Model," Med. Eng. Phys., 34(5), pp. 552–558.

[25] Aour, B., and Damba, N., 2014, "Finite Element Investigation of the Intervertebral Disc Behaviour," Comput. Methods Biomech. Biomed. Eng., 17(Suppl. 1), pp. 58–59.

[26] Ha, S. K., 2006, "Finite Element Modeling of Multi-Level Cervical Spinal Segments (C3-C6) and Biomechanical Analysis of an Elastomer-Type Prosthetic Disc," Med. Eng. Phys., 28(6), pp. 534–541.

[27] Dmitriev, A. E., Cunningham, B. W., Hu, N., Sell, G., Vigna, F., and McAfee, P. C., 2005, "Adjacent Level Intradiscal Pressure and Segmental Kinematics Following a Cervical Total Disc Arthroplasty: An In Vitro Human Cadaveric Model," Spine, 30(10), pp. 1165–1172.

[28] Schwab, J. S., Diangelo, D. J., and Foley, K. T., 2006, "Motion Compensation Associated With Single-Level Cervical Fusion: Where Does the Lost Motion Go?," Spine, 31(21), pp. 2439–2448.

[29] Brodke, D. S., Klimo, P., Jr., Bachus, K. N., Braun, J. T., and Dailey, A. T., 2006, "Anterior Cervical Fixation: Analysis of Load-Sharing and Stability With

Use of Static and Dynamic Plates," J. Bone Jt. Surg. Am. Vol., **88**(7), pp. 1566–1573.

[30] Davies, M. A., Bryant, S. C., Larsen, S. P., Murrey, D. B., Nussman, D. S., Laxer, E. B., and Darden, B. V., 2006, "Comparison of Cervical Disk Implants and Cervical Disk Fusion Treatments in Human Cadaveric Models," ASME J. Biomech. Eng., **128**(4), pp. 481–486.

[31] Anderst, W. J., Baillargeon, E., Donaldson, W. F., III, Lee, J. Y., and Kang, J. D., 2011, "Validation of a Noninvasive Technique to Precisely Measure In Vivo Three-Dimensional Cervical Spine Movement," Spine, **36**(6), pp. E393–E400.

[32] Anderst, W., Baillargeon, E., Donaldson, W., Lee, J., and Kang, J., 2013, "Motion Path of the Instant Center of Rotation in the Cervical Spine During In Vivo Dynamic Flexion-Extension: Implications for Artificial Disc Design and Evaluation of Motion Quality After Arthrodesis," Spine, **38**(10), pp. E594–E601.

[33] Anderst, W. J., Donaldson, W. F., III, Lee, J. Y., and Kang, J. D., 2014, "Continuous Cervical Spine Kinematics During In Vivo Dynamic Flexion-Extension," Spine J., **14**(7), pp. 1221–1227.

[34] Anderst, W. J., 2015, "Bootstrap Prediction Bands for Cervical Spine Intervertebral Kinematics During In Vivo Three-Dimensional Head Movements," J. Biomech., **48**(7), pp. 1270–1276.

[35] Anderst, W. J., Donaldson, W. F., 3rd, Lee, J. Y., and Kang, J. D., 2015, "Three-Dimensional Intervertebral Kinematics in the Healthy Young Adult Cervical Spine During Dynamic Functional Loading," J. Biomech., **48**(7), pp. 1286–1293.

[36] Anderst, W., Donaldson, W., Lee, J., and Kang, J., 2013, "Cervical Disc Deformation During Flexion-Extension in Asymptomatic Controls and Single-Level Arthrodesis Patients," J. Orthop. Res., **31**(12), pp. 1881–1889.

[37] Anderst, W., Donaldson, W., Lee, J., and Kang, J., 2015, "Cervical Spine Disc Deformation During In Vivo Three-Dimensional Head Movements," Ann. Biomed. Eng., **44**(5), pp. 1598–1612.

[38] Wang, S., Xia, Q., Passias, P., Wood, K., and Li, G., 2009, "Measurement of Geometric Deformation of Lumbar Intervertebral Discs Under In-Vivo Weight-bearing Condition," J. Biomech., **42**(6), pp. 705–711.

[39] Wang, S., Xia, Q., Passias, P., Li, W., Wood, K., and Li, G., 2011, "How Does Lumbar Degenerative Disc Disease Affect the Disc Deformation at the Cephalic Levels In Vivo?," Spine, **36**(9), pp. E574–E581.

[40] Li, G., DeFrate, L. E., Park, S. E., Gill, T. J., and Rubash, H. E., 2005, "In Vivo Articular Cartilage Contact Kinematics of the Knee: An Investigation Using Dual-Orthogonal Fluoroscopy and Magnetic Resonance Image-Based Computer Models," Am. J. Sports Med., **33**(1), pp. 102–107.

[41] Fedorov, A., Beichel, R., Kalpathy-Cramer, J., Finet, J., Fillion-Robin, J. C., Pujol, S., Bauer, C., Jennings, D., Fennessy, F., Sonka, M., Buatti, J., Aylward, S., Miller, J. V., Pieper, S., and Kikinis, R., 2012, "3D Slicer as an Image Computing Platform for the Quantitative Imaging Network," Magn. Reson. Imaging, **30**(9), pp. 1323–1341.

[42] Stemper, B. D., Yoganandan, N., and Pintar, F. A., 2003, "Gender Dependent Cervical Spine Segmental Kinematics During Whiplash," J. Biomech., **36**(9), pp. 1281–1289.

[43] Deng, B., Begeman, P. C., Yang, K. H., Tashman, S., and King, A. I., 2000, "Kinematics of Human Cadaver Cervical Spine During Low Speed Rear-End Impacts," Stapp Car Crash J., **44**, pp. 171–188.

[44] Ishii, T., Mukai, Y., Hosono, N., Sakaura, H., Fujii, R., Nakajima, Y., Tamura, S., Iwasaki, M., Yoshikawa, H., and Sugamoto, K., 2006, "Kinematics of the Cervical Spine in Lateral Bending: In Vivo Three-Dimensional Analysis," Spine, **31**(2), pp. 155–160.

[45] Goel, V. K., and Clausen, J. D., 1998, "Prediction of Load Sharing Among Spinal Components of a C5C6 Motion Segment Using the Finite Element Approach," Spine, **23**(6), pp. 684–691.

[46] Hunter, L. Y., Braunstein, E. M., and Bailey, R. W., 1980, "Radiographic Changes Following Anterior Cervical Fusion," Spine, **5**(5), pp. 399–401.

[47] Morishita, Y., Hida, S., Miyazaki, M., Hong, S. W., Zou, J., Wei, F., Naito, M., and Wang, J. C., 2008, "The Effects of the Degenerative Changes in the Functional Spinal Unit on the Kinematics of the Cervical Spine," Spine, **33**(6), pp. E178–E182.

[48] Mummaneni, P. V., Burkus, J. K., Haid, R. W., Traynelis, V. C., and Zdeblick, T. A., 2007, "Clinical and Radiographic Analysis of Cervical Disc Arthroplasty Compared With Allograft Fusion: A Randomized Controlled Clinical Trial," J. Neurosurg. Spine, **6**(3), pp. 198–209.

[49] Ren, C., Song, Y., Xue, Y., and Yang, X., 2014, "Mid- to Long-Term Outcomes After Cervical Disc Arthroplasty Compared With Anterior Discectomy and Fusion: A Systematic Review and Meta-Analysis of Randomized Controlled Trials," Eur. Spine J., **23**(5), pp. 1115–1123.

[50] Verma, K., Gandhi, S. D., Maltenfort, M., Albert, T. J., Hilibrand, A. S., Vaccaro, A. R., and Radcliff, K. E., 2013, "Rate of Adjacent Segment Disease in Cervical Disc Arthroplasty Versus Single-Level Fusion: Meta-Analysis of Prospective Studies," Spine, **38**(26), pp. 2253–2257.

[51] Park, D. K., Lin, E. L., and Phillips, F. M., 2011, "Index and Adjacent Level Kinematics After Cervical Disc Replacement and Anterior Fusion: In Vivo Quantitative Radiographic Analysis," Spine, **36**(9), pp. 721–730.

[52] Pickett, G. E., Rouleau, J. P., and Duggal, N., 2005, "Kinematic Analysis of the Cervical Spine Following Implantation of an Artificial Cervical Disc," Spine, **30**(17), pp. 1949–1954.

[53] Lee, S. H., Im, Y. J., Kim, K. T., Kim, Y. H., Park, W. M., and Kim, K., 2011, "Comparison of Cervical Spine Biomechanics After Fixed- and Mobile-Core Artificial Disc Replacement: A Finite Element Analysis," Spine, **36**(9), pp. 700–708.

[54] Staudt, M. D., Das, K., and Duggal, N., 2016, "Does Design Matter? Cervical Disc Replacements Under Review," Neurosurg. Rev., (epub).